DAB-based Swiss Rectifier for Wide-range Voltage Output with Universal Input

Soichiro Oyoshi
Dept. of Electrical, Electronics and Information Engineering
Nagaoka University of Technology
Nagaoka,Niigata,Japan
s245013@stn.nagaokaut.ac.jp

Keisuke Kusaka
Dept. of Electrical, Electronics and Information Engineering
Nagaoka University of Technology
Nagaoka,Niigata,Japan
kusaka@vos.nagaokaut.ac.jp

Akari Horiuchi
EV System Laboratory, Research Division
Nissan Motor Co., Ltd.
Yokosuka, Kanagawa, Japan
a-horiuchi@mail.nissan.co.jp

Takuru Nakamura
EV System Laboratory, Research Division
Nissan Motor Co., Ltd.
Yokosuka, Kanagawa, Japan
takuru-nakamura@mail.nissan.co.jp

Takayuki Ikari
EV System Laboratory, Research Division
Nissan Motor Co., Ltd.
Yokosuka, Kanagawa, Japan
takayuki-ikari@mail.nissan.co.jp

***Abstract*— The demand for electric vehicle (EV) chargers is increasing alongside the spread of EVs. An onboard charger (OBC) features an AC-DC converter that transforms grid voltage into DC voltage while providing galvanic isolation. For the OBC, a globally compatible voltage input and a wide voltage output range are necessary, all while minimizing size and maximizing efficiency. This paper presents a dual-active bridge converter-based Swiss rectifier (DAB-SR). The proposed topology comprises two dual-active bridge converters connected in series on the primary side and in parallel on the secondary side, together with a Swiss rectifier (SR). The converter operates at unity power factor through DC-link current control applied to the DAB-SR. Simulation results indicate that a sinusoidal input current can be achieved using the current control method employed on the DAB converters.**

Keywords—Swiss Rectifier, DAB converter, Power factor correction

I. INTRODUCTION

In recent years, Electric Vehicles (EVs) have rapidly spread worldwide, supporting the transition to a decarbonized, carbon-neutral society. This trend has resulted in a growing demand for high-performance onboard chargers (OBCs) [1-2], which have an AC-DC converter that converts grid voltage into DC voltage. Besides the common goals of miniaturization and high efficiency in power electronics, the output voltage range has also become a design criterion for an OBC. EV battery voltage is increasing every year and varies from model to model [3]. Furthermore, as the output voltage varies with the state of charge, future EV chargers must operate across a broader range of output voltages [4]. In addition, there are two general specifications for OBCs design [5]: one is the power quality requirement according to the IEEE 519 standard [6]; the other is the safety condition implying that the AC system must be galvanic isolated from the DC vehicle battery, as specified in the UL 2202 standard [7].

A universal input is also required for the OBCs. Each country has different power frequencies and voltages, as a result, automobile companies must design and manufacture OBCs properly for each country or region. This diversity of electrical power systems worldwide raises manufacturing costs; therefore, developing an OBC capable of worldwide input will allow for cost reductions in manufacturing.

The authors are studying the DAB-SR as a three-phase isolated AC-DC topology with universal input. DAB-SR is a combination of the Swiss rectifier (SR) and DAB converters. A Swiss Rectifier has been proposed by J. W. Kolar et al. as a simple AC-DC converter with a simple circuit configuration [8−10]. The Swiss Rectifier is a three-phase buck-type power factor correction (PFC) rectifier with a non-isolated circuit. With the expansion of the Swiss rectifier, circuit topologies incorporating a phase-shifted full-bridge [11−13] or LLC converter [14−15] on the second stage of an unfolding circuit had been developed. However, these topologies encounter limitations regarding the input-output voltage range. The DAB-SR uses the transformer from a DAB converter to achieve isolation, allowing it to function for both boost and buck operations by modulating the phase shift amount. This capability enables the DAB-SR to accommodate a wide range of AC system voltages and DC bus voltages, facilitating global input.

This paper first details the fundamental operation of the dual active bridge (DAB) converter and Swiss rectifier, which are the components of the proposed circuit. It then describes the operating principle of the DAB-SR converter, followed by an assessment of the DAB-SR performance through simulation. The proposed converter enables galvanic isolation, high power factor, and voltage boost/buck operation simultaneously.

II. COMPONENTS OF THE PROPOSED CIRCUIT

DAB-SR combines the Swiss rectifier (SR) and DAB converters. This chapter explains the circuit diagram and operation of the DAB converter and Swiss rectifier, which are the components of the proposed circuit shown in Chapter III below.

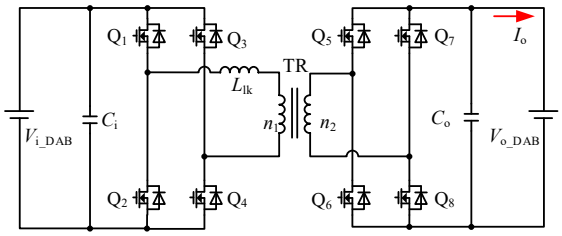

Fig. 1. DAB converter.

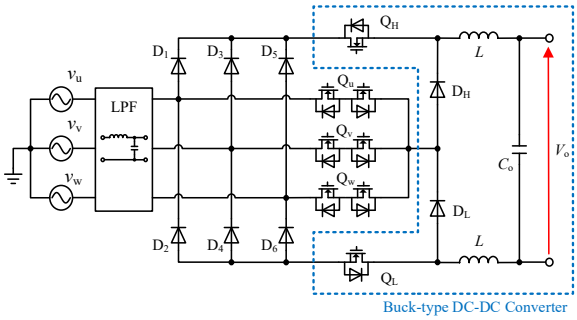

Fig. 2. Swiss rectifier.

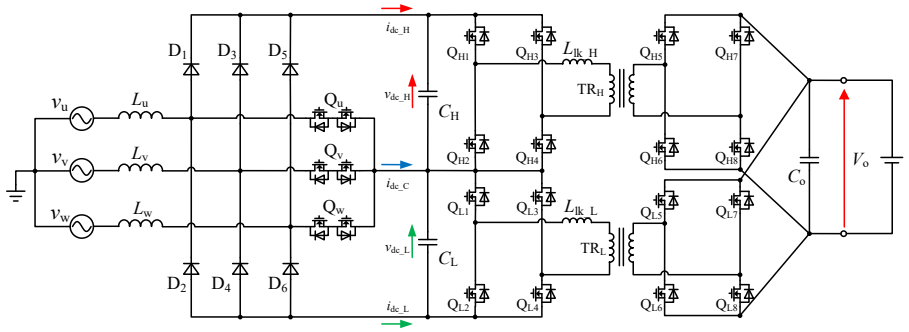

Fig. 3. DAB-SR topology.

A. *DAB Converter*

Fig. 1 shows the circuit configuration of a DAB converter. The DAB converter is a bidirectional DC-DC converter with isolation [11]. The DAB converter consists of a high-frequency transformer responsible for input-output isolation, an inductor in series with the transformer, and two full-bridge inverters. By varying the voltage waveform and phase applied to both ends of the series inductor through the full-bridge inverters on the primary and secondary sides, power can be transmitted in both directions. The phase lag of the current relative to the voltage facilitates zero-voltage switching (ZVS) in the DAB converter; consequently, switching losses can be minimized, and greater efficiency can be achieved.

B. *Swiss Rectifier*

Fig. 2 depicts a Swiss rectifier, which is a unidirectional three-phase buck-type AC-DC converter. The Swiss rectifier comprises a three-phase diode rectifier equipped with a bidirectional switch and a buck-type DC-DC converter linked in the second stage. In a typical diode rectifier, a zero-current period occurs when the voltage across the output capacitor is higher than the input voltage due to the effect of the output capacitor connected in the second stage of the rectifier circuit. During this period, the diode does not turn on and the input current does not flow; consequently, the input current has a distorted waveform with harmonics. In the Swiss rectifier, the three bidirectional switches Q_u, Q_v, and Q_w are switched synchronously at twice the system frequency, and the third harmonic current is passed through a buck-type DC-DC converter. As a result, the conduction angle of the rectifier diode is widened, eliminating the zero-current period of the input current and reducing distortion.

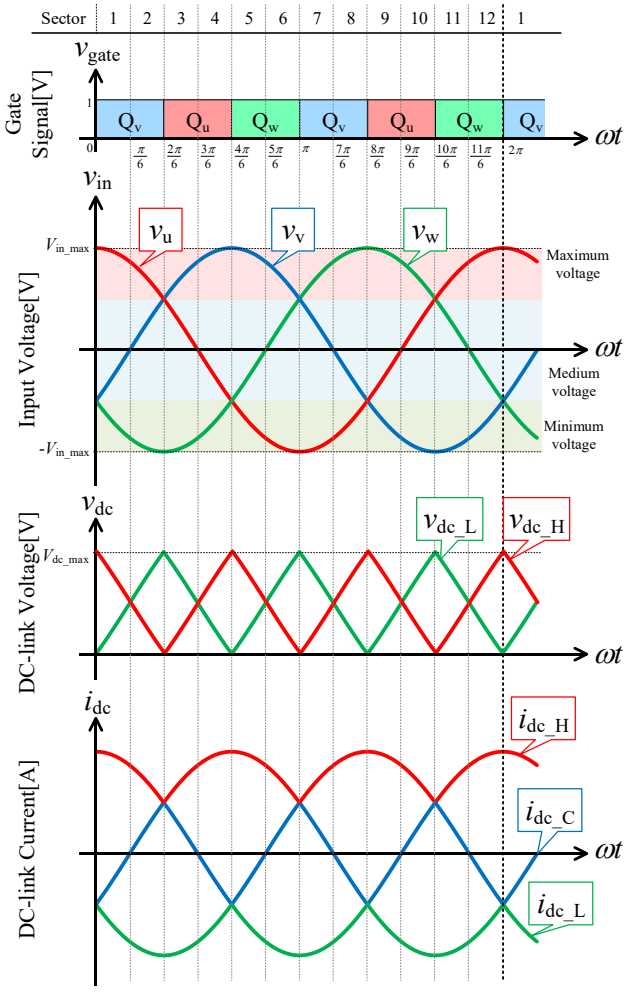

Fig. 4. Waveform of DAB-SR.

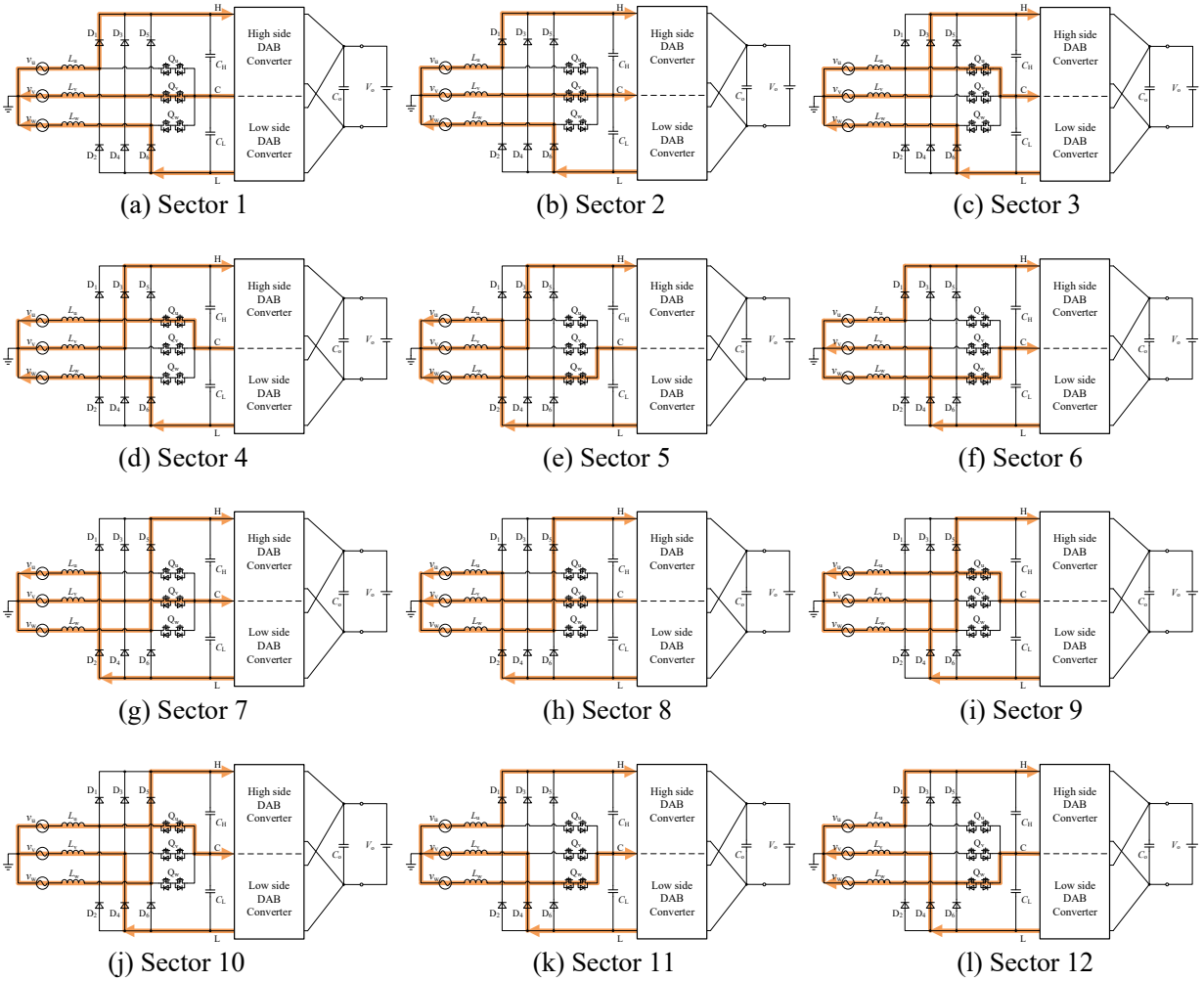

(a) Sector 1 (b) Sector 2 (c) Sector 3

(d) Sector 4 (e) Sector 5 (f) Sector 6

(g) Sector 7 (h) Sector 8 (i) Sector 9

(j) Sector 10 (k) Sector 11 (l) Sector 12

Fig. 5. Current path of input waveform.

III. Proposed Circuit Topology

The proposed circuit (DAB-SR) is illustrated in Fig. 3. DAB-SR is a circuit structure in which two DAB converters replace the buck-type DC-DC converter, achieving both power factor correction and galvanic isolation. The three-phase AC voltage waveforms, the gate signals of the bidirectional switches Q_u, Q_v, Q_w in DAB-SR, and the DC-link voltage/current waveforms are shown in Fig. 4. The three bidirectional switches are switched at the moment when the phase voltage polarity changes. As a result, the three-phase AC voltages shown in (1) are converted to DC-link voltages V_{dc_L} and V_{dc_H}, which are obtained respectively through the difference between the maximum and medium phase voltages and between the minimum and medium phase voltages, as shown in Fig. 4.

$$\begin{cases} v_u = V_{in\_max}\cos(\omega t) \\ v_v = V_{in\_max}\cos(\omega t + \frac{2}{3}\pi) \\ v_w = V_{in\_max}\cos(\omega t - \frac{2}{3}\pi) \end{cases} \quad \cdots\cdots (1)$$

Fig. 5. presents the current path at all sectors. It is imperative to note that the current path in Fig. 5 is unity power factor. As seen from Fig. 5(b), (f), (j) at the moment when input voltage waveforms cross, since v_u and v_v are equal, the voltage at point H and point C are also equal, resulting in a high-side DC-link voltage V_{dc_H} of zero. On the other hand, the high-side DC-link voltage V_{dc_H} is the maximum value V_{dc_max} derived by (2), where V_{in} is the line voltage of the system. The DC-link currents i_{dc_H}, i_{dc_C}, and i_{dc_L} in Fig. 4 are the maximum, medium, and minimum values of the three-phase currents. However, the DC-link voltage and DC-link current shown in Fig. 4 can only be obtained when the power factor is unity. Therefore, an accurate power factor correction is necessary.

$$V_{dc\_max} = \frac{\sqrt{6}}{2} V_{in} \quad \cdots\cdots (2)$$

IV. Control Scheme

As illustrated in Fig. 6, the control block of the DAB-SR consists of several key components. In this paper, power factor correction control is achieved by feeding back the input currents i_{dc_H} and i_{dc_L} of the DAB converter.

The following section will elucidate the methodology for calculating the command values in the input currents i_{dc_H} and i_{dc_L} of the DAB converter. Subsequent to the detection of the three-phase system voltage, standardization is performed by dividing by the system voltage. The command output power

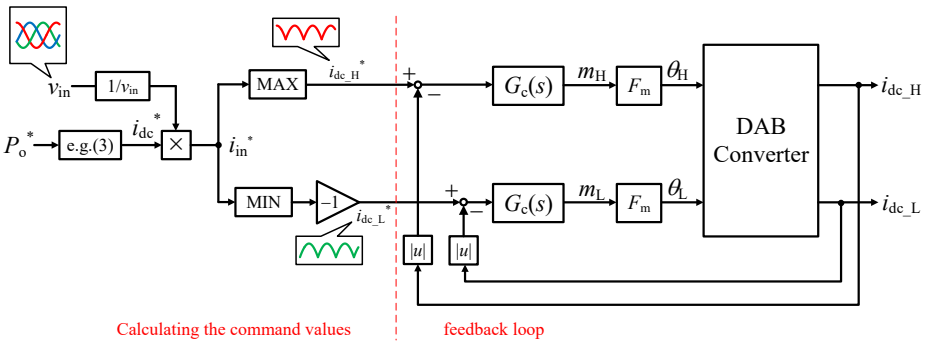

Fig. 6. Control scheme of DAB-SR.

P_o* is then divided by the maximum DC-link voltage to obtain the command current i_{dc}*, as depicted in (3).

$$i_{dc}^{*} = \frac{P_o^{*}}{V_{dc\_max}} \quad \cdots\cdots (3)$$

The command input current is determined by multiplying the standardized three-phase system voltage and the command current i_{dc}*. It should be noted that the command input current is a three-phase signal. By detecting the maximum and minimum values of the command input current, the DC-link current commands i_{dc_H}* and i_{dc_L}* can be obtained.

The subsequent section will describe the feedback unit. The command DC-link currents (i_{dc_H}* and i_{dc_L}*) and the measured DC-link currents (i_{dc_H} and i_{dc_L}) are compared, and the phase shift angles θ_H and θ_L of the DAB converter are modified according to the difference. This adjustment leads to an alteration in the transmit power of the DAB converter and enables indirect control of the DC-link current. Consequently, a sinusoidal current is generated at the input side of the circuit. In this configuration, the compensator $G_c(s)$ assumes the role of a PI controller, and the parameter F_m serves to convert the operating amount m of the PI controller into the phase shift amount of the DAB converter. The expressions for $G_c(s)$ and F_m can be found in (4) and (5), respectively.

$$G_c(s) = k_i + \frac{k_p}{s} \quad \cdots\cdots (4)$$

$$F_m = \frac{m}{\theta} = 4 f_{sw} \quad \cdots\cdots (5)$$

V. Simulation Results

Table 1 shows the parameters of DAB-SR configuration. The input voltage is set to 200 or 400 V to support an universal input. The output voltage V_o is 350 V, simulating the battery voltage of a Nissan LEAF[18]. DAB-SR performs boost and buck operations depending on the system voltage, which are verified in this paper by observing the circuit under both conditions.

A. Input Waveform Analysis

Fig. 7(a) displays the input current waveforms when the input voltage is 200 V (boost operation), and Fig. 7(b) presents the input current waveforms when the input voltage is 400 V (buck operation). It can be seen that the fundamental wave achieved unity power factor for both boost and buck operations, proving that power factor correction is obtained regardless of the operation.

TABLE 1. Parameters of DAB-SR.

Parameters	Symbol	Values	
Input voltage	V_{in}	200/400	[V]
Input frequency	f_i	50	[Hz]
Switching frequency (bidirectional switch)	f_{inj}	100	[Hz]
Switching frequency (DAB converter)	f_{sw}	50	[kHz]
Rated power	P_o^{*}	3.7	[kW]
Output voltage	V_o	350	[V]
Input inductance	L_u, L_v, L_w	800	[μH]
DC-link capacitance	C_H, C_L	5	[μF]
Leakage inductance	L_{lk_H}, L_{lk_L}	11	[μH]
Output capacitance	C_o	500	[μF]

However, ringing occurs in the input current waveforms at the point when the voltage waveforms intersect. The input inductors L_u, L_v, L_w and DC-link capacitors C_H, C_L form an LC filter in the current path, and resonance occurs at the moment when the bidirectional switches Q_u, Q_v, and Q_w are switched. In the u-phase current depicted in Fig. 7(a), the ringing in region A is measured at 5.38 A, while in contrast, it is only 1.05 A in region B. In Fig. 7(b), the ringing for the u-phase current in Region A is 2.87 A, and in Region B, it is 1.19 A. In region A, the ripple is 1.87 times larger at an input voltage of 200V compared to when the input voltage is 400V. In region B, the ripple is 1.13 times larger at an input voltage of 400 V compared to the 200 V condition.

B. DC-link Waveform Analysis

Fig. 8(a) shows the DC-link voltage/current waveforms for an input voltage of 200 V (boost operation) and Fig. 8(b) shows the DC-link voltage/current waveforms for an input voltage of 400 V (buck operation). Compared to the theoretical waveforms in Fig. 4, it can be seen that similar patterns are obtained for both boost and buck operations. However, ringing due to the switching operation of bidirectional switches Q_u, Q_v, and Q_w was observed in the DC-link current during the period when the DC-link voltage was stuck at 0 V.

C. Input Current Harmonics Analysis

Fig. 9 demonstrates the result of the u-phase input current harmonics analysis when the input voltage is 200 V for the boost operation and 400 V for the buck operation. The

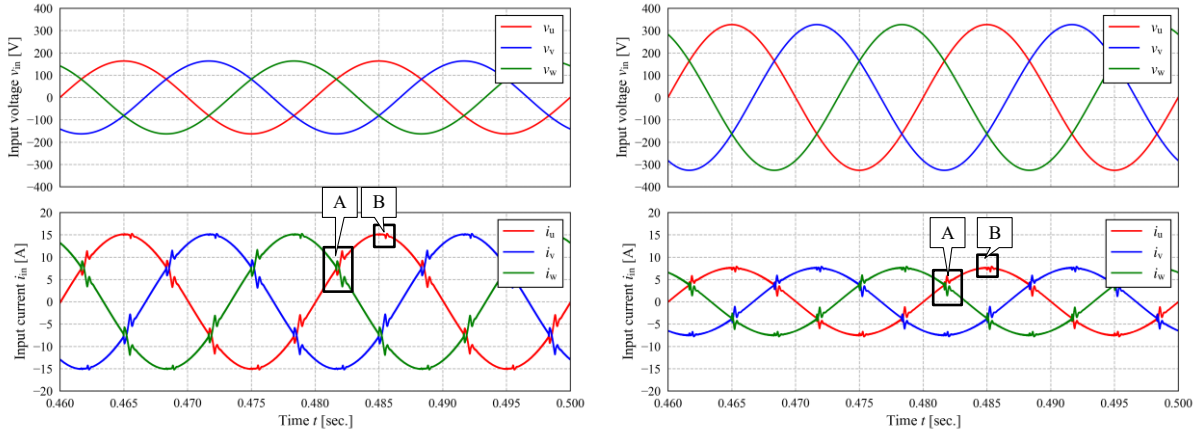

(a) Boost operation (V_{in} = 200V) (b) Buck operation (V_{in} = 400V)

Fig. 7. Input waveform.

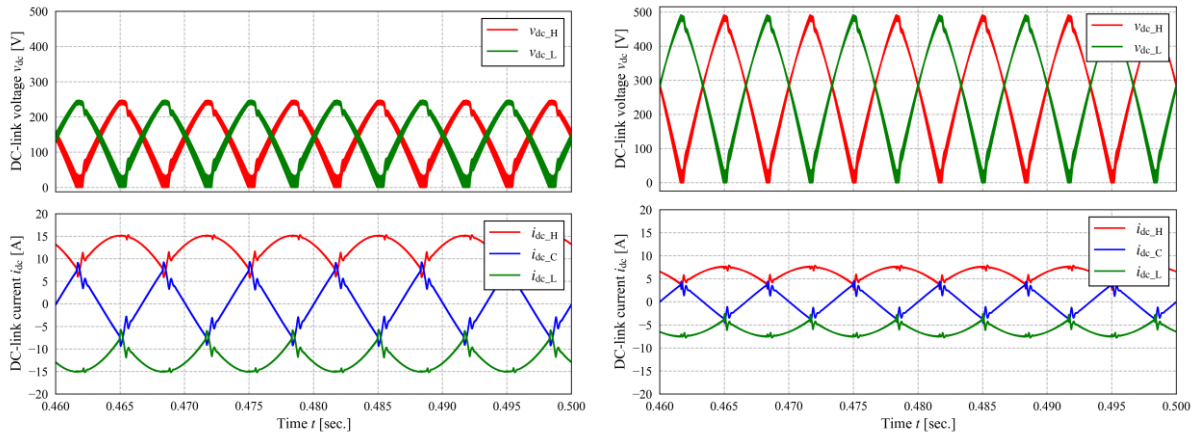

(a) Boost operation (V_{in} = 200V) (b) Buck operation (V_{in} = 400V)

Fig. 8. DC-link waveform.

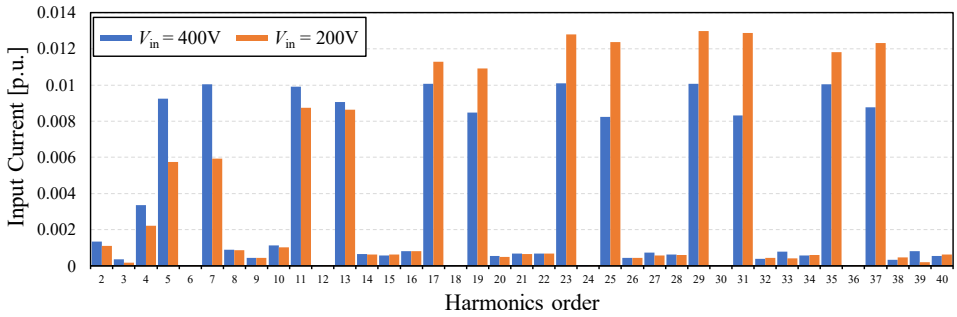

Fig. 9. THD of u-phase input current.

fundamental frequency is 50 Hz, and the amplitude of the fundamental wave is assumed to be 1 p.u. As seen in Fig. 9, the input current contains mostly odd-order harmonics, with particular emphasis on the harmonics at the $(6n \pm 1)$-th order, where n is an integer greater than or equal to 1. Notably, these harmonics are more pronounced. The Total Harmonic Distortion (THD) of the input voltage of 200 V and 400 V are 4.35% and 3.43%, respectively.

VI. Conclusion and Future Work

This paper presents a DAB converter-based Swiss rectifier configuration utilized as a three-phase AC-DC converter with galvanic isolation for OBC development. Simulation results indicate that a sinusoidal input current can be achieved and that boost/buck operation is possible using the current control method employed on the DAB converters. Additionally, favorable outcomes were achieved for the total harmonic distortion (THD) of the input current, which was determined to be less than 5% for both boost and buck operations. However, this study found that ringing caused by polarity switching is superimposed on the input current, resulting in significant current distortion, particularly during boost operation. Applying a commutation to the semiconductor devices on the rectifier side is expected to reduce current distortion. In the future, we plan to mitigate ringing during polarity switching to enhance THD, and to explore a modulation scheme for DAB converters based on soft switching.

REFERENCES

[1] Frede Blaabjerg, "Control of Power Electronic Converters and Systems: Volume 4", Academic Press, 2024.

[2] V. Monteiro, J.L. Afonso, and S. Williamson, "VEHICLE ELECTRIFICATION IN MODERN POWER GRIDS-Disruptive Perspectives on Power Electronics Technologies and Control Challenges-", Elsevier, 2024.

[3] K. Tsutsumi and H. Obara, " Investigation on the Expansion of Output Voltage Range Using a 9-level DAB Converter with Pulse Amplitude Control ", in IEEJ J. Industry Applications, vol. 144, no. 6, pp. 467--475, 2024.

[4] Y. Kinoshita and H. Haga, " Isolated LLC Converter for PEV Charging for Wide-range Voltage Gain using Six-switch Bridge", in IEEJ J. Industry Applications, vol. 140, no. 1, pp. 36-44, 2024.

[5] M. Kumar, S. K. Pramanick, B. K. Panigrahi " Sinusoidal Phase Shift Modulation for V2H Operational Mode in Current-Fed Bidirectional Onboard Charger" in IEEE Transactions on Transportation Electrification, Vol. 10, No.2, pp.3181-3191, June. 2024.

[6] IEEE Recommended Practice and Requirements for Harmonic Control in Electric Power Systems, Standard 519-2014 Revis. IEEE Std 519-1992, Jun. 2014, pp. 1–29.

[7] UL-2202 Standard for Electric Vehicle (EV) Charging System Equipment| Standards Catalog. Accessed: Jan. 20, 2023. [Online]. Available:https://standardscatalog.ul.com/standards/en/standard_2202_2

[8] M. Kumar, S. K. Pramanick, B. K. Panigrahi " Sinusoidal Phase Shift Modulation for V2H Operational Mode in Current-Fed Bidirectional Onboard Charger" in IEEE Transactions on Transportation Electrification, Vol. 10, No.2, pp.3181-3191, June. 2024.

[9] J. W. Kolar and T. Friedli, " The Essense of Three-Phase PFC Rectifier Systems ", in Proc. 33rd IEEE Int. Telecom. Energ. Conf (INTELEC 2011), 9-13, pp. 1-27, Oct. 2011.

[10] J. W. Kolar, M. Hartmann and T. Friedli, " Three-Phase Unity Power Factor Mains Interfaces of High Power EV Battery Charging Systems", in Power Electronics for Charging Electric Vehicles ECPE Workshop, Mar. 2011.

[11] T. B. Soeiro, T. Friedli and J. W. Kolar, "Swiss rectifier — A novel three-phase buck-type PFC topology for Electric Vehicle battery charging" in 27th Applied Power Electronics Conference and Exposition (APEC), Feb. 2012.

[12] X. Wang, B. Zhang, S. Xie and K. Xu, "A Soft Switching Swiss Rectifier Based on Phase-Shifted Full-Bridge Topology" in Proc. IEEE Int. Power Electron. Conf. Expo., pp. 1-6. April. 2018.

[13] B. Zhang, S. Xie, X. Wang and J. Xu, " Modulation Method and Control Strategy for Full-Bridge-Based Swiss Rectifier to Achieve ZVS Operation and Suppress Low-Order Harmonics of Injected Current", in IEEE Transactions on Power Electronics, vol. 35, no. 6, pp. 6512 - 6522, June. 2020.

[14] B. Zhang, S. Xie, Z. Li, P. Zhao and J. Xu, "An Optimized Single-Stage Isolated Swiss-Type AC/DC Converter Based on Single Full-Bridge With Midpoint-Clamper", in IEEE Transactions on Power Electronics, vol. 36, no. 10, pp. 11288 - 11297, Oct. 2021.

[15] C. Jingke, X. Junzhong, C. Kaihong, B. Yuxuan, Z. Yuxin and W. Yong, "Output Voltage Ripple Suppression Strategy for Light DC-link Capacitor DC-Type EV Charger", in IEEE 10th International Power Electronics and Motion Control Conference (IPEMC2024-ECCE Asia), May. 2024.

[16] X. Li, J. Sun, L. Guo, M. Gao, H. Hu and M. Xu, " A Three-Phase Single-Stage ac/dc Converter Based on Swiss Rectifier and Three-Level LLC Topology ", in IEEE Transactions on Power Electronics, vol. 38, no. 2, pp. 1958 - 1972, Feb. 2023.

[17] K. Hirachi, "Fundamentals and Applications of Soft-Switching", IEEJ, 2022.

[18] NISSAN LEAF spec-sheet. Accessed: Mar. 26, 2025. [Online]. https://www-asia.nissan-cdn.net/content/dam/Nissan/jp/vehicles/leaf/2409/pdf/leaf_specsheet.pdf?adobe_mc=MCMID%3D04987294835242204230851124438248292478%7CMCORGID%3D0BCEE1CE543D41F50A4C98A5%2540AdobeOrg%7CTS%3D1742950892